Measuring Practical Coil Array Performance with Respect to Ultimate Intrinsic SNR: A Tool for Array Design and Assessment

R. Lattanzi[1,2], A. K. Grant[2], M. A. Ohliger[1,2], D. K. Sodickson[1,2]

[1]Division of Health Science and Technology, Harvard-MIT, Cambridge, MA, United States, [2]Radiology, Beth Israel Deaconess Medical Center, Boston, MA, United States

Introduction

As the number of available receiver channels on modern MR systems increases, increasing attention will be paid to the design and performance of many-element RF coil arrays. Questions regarding the balance of coil-noise and sample-noise or the suitability of any particular array design for parallel imaging– already areas of great practical interest to coil designers – promise to take on new significance as the number of elements increases. In this context, it would be useful to have a concrete metric of coil performance, in order not only to compare different designs but also to determine how much room for improvement there may be in any particular design. Recent studies have shown that there is an inherent electrodynamic limitation to the achievable SNR for any physically realizable coil array (assuming sample-dominated noise), and have modeled the behavior of ultimate intrinsic SNR either in the absence [1] or in the presence [2,3] of parallel acceleration. In [1], coil performance maps were also presented, in which the actual SNR of particular coils was compared with the appropriately scaled ultimate intrinsic SNR for a particular phantom and image plane geometry. In this work, we extend the computation of coil performance maps to include the effects of parallel imaging. We compute the ultimate SNR at each point within a central cross-section of a cylindrical phantom for a variety of acceleration factors, and express the actual SNR, measured with a particular eight-element coil array in a phantom with the same geometry, as a percentage of the ultimate achievable value. Such coil performance maps may of course be generated for arbitrary coil arrays and object/image geometries, and they may ultimately be used as absolute references for coil design optimization.

Materials and Methods

The best possible SNR can be found by substituting coil sensitivities in the image reconstruction algorithm with a complete set of basis functions that are valid

solutions of Maxwell's equations. The electric field associated to these basis functions is used to compute the noise-resistance matrix Ψ which specifies the noise power associated with any linear combination of coil sensitivities. Using the weak SENSE reconstruction algorithm for parallel MRI [4], which has unit sensitivity at the pixel of interest and zero at the aliased positions, the ultimate intrinsic SNR can be expressed as:

$$\text{SNR}_{\text{intr}}^{\text{ult}} = \sqrt{2}\,\omega\,M_0 \Big/ \sqrt{4 K_B T_S \left(\mathbf{B}^\dagger \Psi^{-1} \mathbf{B}\right)^{-1}},$$

where ω is the Larmor frequency, M_0 is the equilibrium magnetization, k_B is Boltzmann's constant, T_S is the temperature of the sample and $\mathbf{B}$ is the encoding matrix as defined in [2].

The net field inside a cylindrical-shaped uniform phantom was expressed as a linear combination of cylindrical harmonics (having the form $e^{ikz}e^{im\phi}J_m(k'\rho)$, with integer m and suitable values of k and k') satisfying Maxwell's equations in a source free medium [5]. A coronal section passing through the center of a cylinder was divided in a grid of 5184 squares of side 3.125 mm, arranged in a 108 by 48 mesh (Fig. 1) and the ultimate intrinsic SNR was computed at each point using Mathematica (Wolfram Research, USA). The electrical properties of an SNR phantom of the same cylindrical shape (USA Instruments Inc., 3.3685 g/L NiCl$_2$ 6H$_2$O, 2.4 g/L NaCl) were used in the algorithm. The phantom was scanned along the same coronal plane on a GE 1.5 TwinSpeed system (GE Medical Systems, USA), using a linear eight-element coil array shown in Fig. 1 and described more fully in Ref. [6]. The total area of the array was 13.3 cm x 27.3 cm, providing full coverage of the chosen FOV. A gradient echo pulse sequence with a TR of 1 s and a
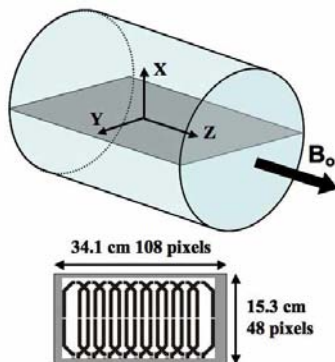
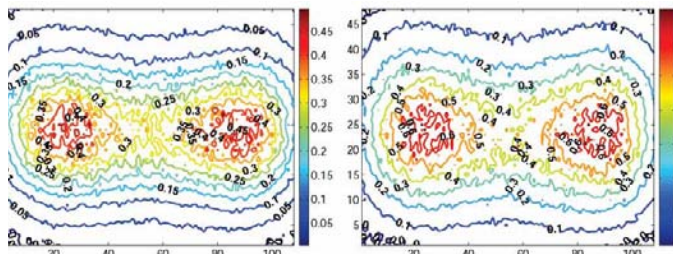Figure 1: Schematic diagram of the FOV, the geometry and the coil array used

TE of 5.1 ms was chosen to minimize T1 and T2 effects. The pixel size was the same as in the simulation, the slice thickness was 1 mm and the flip angle was 10°. The same slice was sequentially acquired 112 times and reconstructed off-line using a Cartesian SENSE algorithm. An SNR image was then generated, computing the SNR at each pixel as its mean value along the 112 replicas, divided by the standard deviation in the same interval. The ultimate SNR values were scaled to account for the sequence parameters, in order to compare the experimental data with the simulated data:

$$\text{SNR} = \text{SNR}_{\text{intr}}^{\text{ult}}\left(V\sin(\theta)\sqrt{N_{\text{acq}}\text{NEX}}\Big/\text{NF}\sqrt{2\text{BW}}\right),$$

where V is the voxel volume, θ is the flip angle, N_{acq} is the number of acquired k-space data points, NEX is the number of repetitions, NF is the noise figure of the preamplifiers and BW is the bandwidth. Performance maps for the coil array were computed as the ratio of the actual SNR to the scaled ultimate SNR, as a function of position inside the sample of interest, for various acceleration factors.

Figure 2: Coil performance map showing the fraction of ultimate SNR achievable for unaccelerated (left) and 2-fold accelerated (right) studies with the 8-element array

Results and Discussion

The choice of basis functions was found to have a significant influence on the convergence behavior and the numerical tractability of the ultimate intrinsic SNR calculations, and this motivated our choice of cylindrical harmonic functions matched to the geometry of the phantom, as opposed to the plane wave [1,2] or spherical harmonic [3] bases used previously. The simulation of ultimate intrinsic SNR converged with 200 cylindrical harmonic modes (assuming, for computational convenience, a plane-wave dependence in the z-direction, which should capture the dominant behavior for long cylinders. Exploration of the evanescent-wave effects in the z direction is underway). The average SNR for the experimental MR images was 12 in the fully sampled reconstruction and 8 in the 2-fold undersampled one (with comparatively low values deliberately chosen to eliminate system instabilities from the replica-based SNR measurements). Figure 2 shows coil performance maps for acceleration factors R = 1 and 2. In the unaccelerated case the SNR was always less than 45% of the optimum, whereas in the case of 2-fold acceleration, although the overall value of the SNR was lower, performance of the coil array reached 60% in the regions of high signal. The lateral elements of the array performed better than the central elements. Otherwise, as expected, the performance is generally higher in the center, as the ultimate SNR decreases rapidly from the edge of the phantom toward the middle.

Conclusions

We have described a method to evaluate the absolute performance of any particular coil array. This procedure can be used to improve the design of receiver coils for sequential or parallel imaging applications. Future investigations will evaluate larger numbers of array elements and higher accelerations.

References

[1] Ocali O, et al (1998) MRM 39: 462-473 [2] Ohliger MA, et al (2003) MRM 50: 1018-1030 [3] Wiesinger F, et al (2004) MRM 52: 953-964
[4] Pruessmann KP, et al (1998) MRM 42: 952-962   [5] Jackson JD, Classical Electrodynamics (1999)   [6] Sodickson DK et al, ISMRM 2003, 469.